JOURNAL OF BACTERIOLOGY, Jan. 2009, p. 641–650 Vol. 191, No. 2
0021-9193/09/$08.00+0 doi:10.1128/JB.01029-08
Copyright © 2009, American Society for Microbiology. All Rights Reserved.

Structure-Activity Relationship of Gelatinase Biosynthesis-Activating Pheromone of *Enterococcus faecalis*▽

Kenzo Nishiguchi,[1] Koji Nagata,[2] Masaru Tanokura,[2] Kenji Sonomoto,[1,3] and Jiro Nakayama[1]*

Department of Bioscience and Biotechnology, Faculty of Agriculture, Graduate School, Kyushu University, Fukuoka 812-8581, Japan[1]; Department of Applied Biological Chemistry, Graduate School of Agriculture and Life Sciences, University of Tokyo, Tokyo 113-8657, Japan[2]; and Department of Functional Metabolic Design, Bio-Architecture Center, Kyushu University, Fukuoka 812-8581, Japan[3]

Received 25 July 2008/Accepted 28 October 2008

The expression of pathogenicity-related extracellular proteases, namely, gelatinase and serine protease, in *Enterococcus faecalis* is positively regulated by a quorum-sensing system mediated by an autoinducing peptide called gelatinase biosynthesis-activating pheromone (GBAP). GBAP is an 11-amino-acid-residue cyclic peptide containing a lactone linkage. To study the structure-activity relationship of GBAP, we synthesized a series of GBAP analogues and evaluated their activities by a gelatinase-inducing assay and newly developed receptor-binding assays in which fluorescence-labeled peptides bound onto the FsrC-overexpressing *Lactococcus lactis* cell surface were observed by fluorescent microscopy and quantified by using a fluorophotometer. Alanine-scanning analysis of GBAP showed that the entire ring region was involved in the GBAP agonist activity, while side chains of the tail region were not strictly recognized. The alanine substitution of Phe^{7} or Trp^{10} almost abolished their receptor-binding abilities and GBAP agonist activities, suggesting that these two aromatic side chains are strongly involved in receptor interaction and activation. Furthermore, the Trp^{10} substitution with natural and unnatural aromatic amino acids, except pentafluorophenylalanine, caused no loss of agonist activity. This suggested the importance of a negative electrostatic potential created by an π-electron cloud on the aromatic ring surface. Structural analysis of GBAP with nuclear magnetic resonance spectroscopy revealed that the ring region adopted a hairpin-like fold and was tightly packed into a compact form. The side chain of Trp^{10} was partially buried in the core structure, contributing to the stabilization of the compact form, while that of Phe^{7} was extended from the core structure into the solvent and was probably directly involved in receptor binding.

Enterococcus faecalis is an intestinal commensal found in humans and other animals. However, it occasionally causes opportunistic infections, e.g., bacteremia, endocarditis, urinary tract infection, and endophthalmitis (15). In addition, the recent appearance of antibiotic-resistant and, notably, vancomycin-resistant enterococci poses a serious clinical problem (10, 21, 25). Several virulence-related factors in *E. faecalis* have been described, including cytolysin (5), aggregation substance (Agg), enterococcal surface protein (Esp), and two extracellular proteases, namely, gelatinase and serine protease (24, 34).

Gelatinase and serine protease are encoded in the *gelE-sprE* operon, whose transcription is positively regulated by the *fsr* quorum-sensing system (31, 32). The *fsr* locus is composed of four genes, namely, *fsrA*, *fsrB*, *fsrC*, and *fsrD* (28). Furthermore, in this *fsr* system, a cyclic peptide named gelatinase biosynthesis-activating pheromone (GBAP) acts as an autoinducing peptide (26, 27). GBAP is an 11-amino-acid-residue cyclic peptide with a lactone linkage between the α-carboxyl group at the C-terminal methionine residue and a hydroxyl group of the serine residue at the third position from the N terminus (26) (Fig. 1). It was previously proposed that FsrD, which is the propeptide of GBAP, is processed and cyclized by FsrB and eventually maturates into GBAP (28). GBAP accumulates outside the cell, and when the concentration of GBAP exceeds approximately 1 nM, a two-component signal transduction cascade of FsrC-FsrA is triggered.

Quorum sensing has recently been considered to be a target for the development of antipathogenic agents (1, 22, 30, 33). Two main approaches may be used to develop an inhibitor against GBAP-mediated quorum sensing in *E. faecalis*. One approach is to screen natural compounds. Recently, it was demonstrated that a peptide antibiotic, siamycin I, produced by *Streptomyces* sp. strain Y33-1 shows potent and specific inhibitory activity against GBAP-mediated quorum sensing at sublethal concentrations (29). The other approach is to design an antagonist by using the knowledge regarding the structure-activity relationship (SAR) of GBAP, as was previously done for staphylococcal *agr* quorum sensing mediated by thiolactone-autoinducing peptide (AIP) (11, 18, 19, 23). Nakayama et al. (27) previously reported that the linear form of GBAP has no gelatinase-inducing activity, as is the case with staphylococcal thiolactone-containing AIPs (23). Furthermore, it was previously reported that N-terminally acetylated GBAP shows slightly lower levels of gelatinase-inducing activity than does GBAP (27). However, little knowledge on the SAR of GBAP is currently available.

In the present study, we performed detailed SAR studies of GBAP by using a newly constructed receptor-binding assay

* Corresponding author. Mailing address: Laboratory of Microbial Technology, Department of Bioscience and Biotechnology, Faculty of Agriculture, Graduate School, Kyushu University, 6-10-1 Hakozaki, Higashi-ku, Fukuoka 812-8581, Japan. Phone: 81-92-642-3020. Fax: 81-92-642-3021. E-mail: nakayama@agr.kyushu-u.ac.jp.

▽ Published ahead of print on 7 November 2008.

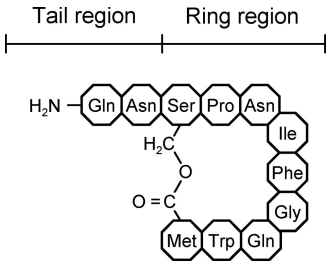

FIG. 1. Structure of GBAP.

system and a gelatinase-inducing bioassay. It was demonstrated that two aromatic amino acid residues, namely, Phe^7 and Trp^{10}, in the ring region of GBAP are strongly involved in the GBAP-FsrC interaction and subsequent FsrC activation. Furthermore, we performed structural analysis of GBAP by nuclear magnetic resonance (NMR) spectroscopy to clarify its solution conformation; we found that Trp^{10} contributed to the stabilization of the compact form of the GBAP ring region.

MATERIALS AND METHODS

Bacterial strains and growth conditions. The strains used in this study are listed in Table 1. *E. faecalis* OG1RF (9) was used as the standard gelatinase-positive strain to examine the GBAP agonist/antagonist activity of each synthetic peptide. *E. faecalis* OU510 has an amber mutation in *fsrB*, resulting in a lack of GBAP biosynthesis. This strain was used as the responder strain for the GBAP agonist activity assay because gelatinase production in this strain completely depends on exogenously added GBAP (28). All *E. faecalis* strains were cultured in 36.4 g/liter Todd-Hewitt broth (THB) (Oxoid, Basingstoke, Hampshire, United Kingdom) at 37°C with gentle agitation. *Lactococcus lactis* NZ9000 (17) carrying pNZfsrC-his6 was cultivated in 42.5 g/liter M17 medium (Merck, Darmstadt, Germany) supplemented with 0.5% glucose and 10 μg ml^{-1} of chloramphenicol (GM17MC) at 30°C without agitation.

Peptide synthesis. All the cyclic peptides used in this study, except disulfide-GBAP, were synthesized according to a previously developed scheme in which the linear peptides were dehydrated between the hydroxyl group of Ser^3 and the carboxyl group at the C terminus (27). The protected linear peptides were manually synthesized by a solid-phase peptide synthesis method using *p*-alkoxybenzoyl alcohol resin (Wang resin) (Kokusan Kagaku, Tokyo, Japan) as a solid support (4). The side-chain-protecting groups of the 9-fluorenylmethoxy carbonyl amino acids were as follows: the trityl (Trt) group for asparagine [Asn(Trt)], cysteine [Cys(Trt)], homoserine [Hse(Trt)], and glutamine [Gln(Trt)]; the *t*-butyl (tBu) group for serine [Ser(tBu)]; and the *t*-butoxycarbonyl (Boc) group for diaminopropionic acid [Dpr(Boc)] and tryptophan [Trp(Boc)]. The N-terminal-protecting group of amino acids for the cyclization reaction was the benzyloxycarbonyl (Z) group for glutamine [Z-Gln(Trt)], asparagine [Z-Asn(Trt)], and serine [Z-Ser(tBu)]. The N-terminally protected linear peptides were obtained by exposure to 86.5% trifluoroacetic acid (TFA), 5% phenol, 5% water, 2.5% ethanedithiol, and 1% triisopropylsilane, and subsequent cyclization was performed using benzotriazole-1-yl-oxy-tris-pyrrolidino-phosphonium-hexafluorophosphate as previously described (27). Finally, mature cyclic peptides were cleaved from N-terminally protected cyclic peptides by exposure to a solution containing 76% TFA, 7.5% thioanisole, 7.5% ethanedithiol, 7.5% *m*-cresol, and 1.5% TFA anhydride.

To synthesize *N*-acetyl $desQ^1$-GBAP and *N*-acetyl $desQ^1N^2$-GBAP, 240 μg of $desQ^1$-GBAP and 70 μg of $desQ^1N^2$-GBAP were dissolved in a solution containing 200 μl acetic anhydride and 200 μl pyridine and kept overnight at 37°C.

Disulfide-GBAP was synthesized by incubating 25 mg of a deprotected linear peptide, H_2N-Gln-Asn-Cys-Pro-Asn-Ile-Phe-Gly-Gln-Trp-Cys-OH, with 10% acetic acid (25 ml) (pH 7.8) and 0.1 M potassium ferricyanide (520 μl) at 37°C for 20 min.

Fluorescence-labeled peptides for the receptor-binding assay were prepared by reacting unlabeled peptides with fluorescein-4-isothiocyanate (FITC; Dojindo, Kumamoto, Japan) (13). Each synthetic peptide (GBAP [167.9 μg] and F^7A-GBAP [51.7 μg] or W^{10}A-GBAP [82.5 μg]) was dissolved in 100 μl of 50 mM Tris-HCl (pH 7.8) and mixed with an equal volume of 1 mg ml^{-1} FITC stock solution (50 mM Tris-HCl, pH 7.5). The reaction mixtures were incubated separately for 1 h at room temperature.

All crude peptides were purified by reverse-phase high-performance liquid chromatography (RP-HPLC) using an Inertsil octadecyl silane-3 column (5 μm, 4.6 by 150 mm; GL Sciences Inc., Tokyo, Japan) after cleanup of the reaction mixture with a Sep-pak C_{18} cartridge column (Waters, MA). The HPLC conditions that were employed were as follows: the solvent system was water containing 0.1% TFA (A solution) and acetonitrile containing 0.1% TFA (B solution), elution was performed with a linear gradient of 20 to 60% B solution for 40 min, the flow rate was 1 ml min^{-1}, and UV detection was done at 220 nm. The molecular weights of all resulting peptides were ascertained by electrospray ionization mass spectroscopy (AccuTOF T100LC; Jeol, Tokyo, Japan).

GBAP agonist and antagonist assay. For the GBAP agonist assay, *E. faecalis* OU510 was used as the responder strain. The use of this strain allows the measurement of GBAP agonist activity in each tested peptide without the additive effect of endogenously produced GBAP. A culture of *E. faecalis* OU510 grown overnight was inoculated at an optical density at 660 nm (OD_{660}) of 0.02 into 5 ml of THB medium containing 10 nM of each synthetic tested peptide and then grown at 37°C with gentle agitation. *E. faecalis* OU510 cells grown in THB medium containing 10 nM of GBAP served as the control. The culture supernatant was collected 5 h after the inoculation, and the gelatinase activity induced in the supernatant was measured using azocoll (<50 mesh; Calbiochem, San Diego, CA) as the substrate for gelatinase according to a protocol described previously (20, 26). Briefly, 40 μl of the culture supernatant was added to 0.8 ml of the azocoll substrate solution and incubated for 4 h at 37°C on a shaker (170 rpm) (SN-30B; Nissin Scientific Corp., Tokyo, Japan). The mixture was centrifuged at 20,000 × *g* for 5 min, and the OD_{540} of the supernatant was measured.

E. faecalis OG1RF was used as the responder strain for the GBAP agonist/antagonist assay. In general, this strain produces approximately 10 nM GBAP in the late exponential phase of culture. Since OG1RF endogenously produces

TABLE 1. Strains and plasmids used in this study

Strain or plasmid	Genotype	Phenotype	Reference or source
Strains			
Enterococcus faecalis OG1RF	*fsrA*$^+$ *fsrB*$^+$ *fsrD*$^+$ *fsrC*$^+$ *gelE*$^+$ *sprE*$^+$	Gelatinase positive, GBAP positive; useful for GBAP agonist/antagonist assay	9
Enterococcus faecalis OU510	*fsrA*$^+$ *fsrB* (amber mutation at the position corresponding to Leu-65) *fsrD*$^+$ *fsrC* *gelE*$^+$ *sprE*$^+$	Gelatinase negative, GBAP negative; useful for GBAP agonist activity	28
Lactococcus lactis NZ9000	MG1363 derivative; *pepN*::*nisRK*	Useful as a host for nisin-controlled expression systems	17
Plasmids			
pNZ8048	*nisA* promoter$^+$ NcoI site$^+$ MCS$^+$ terminator; pSH71 replicon; Cm^r	Translational fusion vector for nisin-controlled expression in *L. lactis*	17
pNZfsrC-his6	pNZ8048 derivative containing hexahistidine-tagged *fsrC* associated with *nisA* promoter	Nisin-inducible FsrC-His_6 overexpression in *L. lactis*	This study

GBAP, which autoinduces gelatinase production, not only agonist activity but also antagonist activity can be simultaneously examined in this assay; an activity higher than 100% means agonist activity, and an activity lower than 100% means antagonist activity. A culture of *E. faecalis* OG1RF grown overnight was inoculated to an OD_{660} of 0.02 into 5 ml of THB medium containing 1,000 nM of each synthetic peptide and was then grown at 37°C with gentle agitation. *E. faecalis* OG1RF grown in THB medium containing 1,000 nM of GBAP served as a control. The culture supernatant was collected 5 h after the inoculation, and the gelatinase activity induced in the supernatant was measured as described above.

Overexpression of FsrC on *Lactococcus lactis*. Plasmid pNZ8048 is a vector allowing the nisin-controlled expression of genes of interest; this vector was used for the expression of hexahistidine-tagged *fsrC* (8, 17) (Table 1). An *fsrC* gene fragment was PCR amplified using KOD Plus DNA polymerase (Toyobo, Osaka, Japan) with *E. faecalis* OG1RF chromosomal DNA as the template and the following primers: fsrC-his6-F1 (5′-CCCTGAATCATGATTTTGTCGTTATTAGC-3′) and fsrC-his6-R (5′-AATACCGAGCTCTTAATGATGATGATGATGATGTTCGTTAACAACTTTTTTACTG-3′) The latter sequence contains a SacI site (indicated by underlining) for cloning. The amplified fragment was used as the template for the reamplification of *fsrC* gene fragments with the following primers: fsrC-his6-F2 (5′-CCGAATCTGCAGAAATGATTTTGTCGTTA-3′) and fsrC-his6-R. The former sequence has a PstI site (indicated by underlining) for cloning. The obtained fragments and pNZ8048 were digested with the restriction enzymes PstI (Takara Bio Inc., Shiga, Japan) and SacI (Roche, Indianapolis, IN) and then both ligated by using the Ligation-high kit (Toyobo). The resulting plasmid, pNZfsrC-his6, was introduced into *Lactococcus lactis* NZ9000 by electroporation according to previously developed methods (16). The transformed *fsrC* gene was sequenced to confirm that no mutation had occurred. *L. lactis* NZ9000 harboring vector pNZ8048 and without the *fsrC*-His_6 gene was used as the control. A culture of recombinant *L. lactis* NZ9000 cells grown overnight was inoculated into 200 ml of fresh GM17MC. After the culture reached an OD_{600} of 0.5, nisin A (Sigma-Aldrich, Inc., St. Louis, MO) dissolved in water and adjusted to pH 3.0 with HCl was added to achieve a final concentration of 10 ng ml^{-1} for the induction of the *fsrC*-His_6 gene. The culture was maintained for 3 h for the expression of FsrC-His_6.

To confirm the overexpression of FsrC-His_6, the cells were harvested, suspended in 50 mM Tris-HCl (pH 7.5), and treated with 25 μg ml^{-1} of lysozyme for 30 min at 37°C. The resulting spheroplasts were disrupted using an ultrasonic disintegrator. The membrane fraction was separated by ultracentrifugation at 125,000 × *g* for 90 min and sodium dodecyl sulfate-polyacrylamide gel electrophoresis, followed by Western blot analysis using anti-histidine tag antibody to detect FsrC-His_6. Western blot analysis was performed using the Penta-His HRP conjugate kit (Qiagen GmbH, Hilden, Germany) according to the manufacturer's protocol.

Fluorescence-based receptor-binding assay. After the induction of recombinant *L. lactis* cells, the cells were harvested and washed with 50 mM Tris-HCl (pH 7.8), and the cell concentration was adjusted to an OD_{600} of 10. One hundred microliters of cell suspension was added to a 1.5-ml tube containing an equal volume of 2 μM of each FITC-labeled peptide. The mixture was then incubated for 1 h at 30°C with shaking (120 rpm) (SN-30B; Nissin Scientific Corp.). Subsequently, the mixture was centrifuged at 6,000 × *g* for 3 min, and the cell pellet was washed thoroughly three times with 50 mM Tris-HCl (pH 7.8). The washed cells were resuspended in 100 μl of 50 mM Tris-HCl (pH 7.8) and observed under a fluorescent microscope (Eclipse 80i; Nikon, Tokyo, Japan). To quantify the fluorescence-labeled peptides bound to *L. lactis* transformant cells, the cell suspension was added into 2 ml of water in the microcell containing 0.25% (vol/vol) Triton X-100 and 2.5 μM of 5-dimethylamino-1-naphthalenesulfonyl (DNS)-phosphatidyl-ethanolamine as the internal standard. The fluorescence intensity of the mixture was measured at an absorbance (emission wavelength) of 520 nm, with excitation wavelengths ranging from 300 to 500 nm. A fluorophotometer (F-7000; Hitachi, Tokyo, Japan) (the excitation wavelengths of FITC and DNS are 495 nm and 340 nm, respectively) was used for this purpose. The fluorescence intensity of FITC was normalized to that of DNS-phosphatidyl-ethanolamine.

NMR spectroscopy. ^1H-^1H two-dimensional NMR data, i.e., DQF-COSY (double-quantum filtered-correlation spectroscopy), TOCSY (total correlation spectroscopy) (50-ms mixing time), and NOESY (nuclear Overhauser effect spectroscopy) (100-, 200-, 300-, 400-, and 500-ms mixing times) for 1.5 mM GBAP dissolved in 90% H_2O–10% D_2O (vol/vol) (pH 6.0, direct meter reading) were collected at 10°C using a Unity Inova 500 spectrometer (Varian, CA). ^1H-^{15}N two-dimensional NMRs (natural-abundance ^1H-^{15}N HSQC [heteronuclear single-quantum coherence]) of 1.5 mM wild-type and F^7A- and $W^{10}A$-GBAPs dissolved in the same solution described above were collected at 10°C using a Unity Inova 600 spectrometer (Varian). The acquired NMR data were processed, visualized, and peak picked with the software packages NMRPipe, NMRDraw (6), and SPARKY (12), respectively. Sequential assignments (35) were accomplished. Structure calculations were performed with the program CYANA (14), with 105 distance restraints and 8 ϕ angle restraints obtained from NOESY (200-ms mixing time) and DQF-COSY, respectively. A total of 20 structures were selected from 100 calculated structures on the basis of their values of CYANA target function and were then subjected to restrained energy minimization in the CNS program (3) with the ester bond restrain between Ser^3 and Met^{11} in addition to the NMR-derived restrains. As a result, an ensemble of the 10 lowest-energy structures was retained. The molecular structure was visualized with the program PyMOL (7).

CD spectroscopy. Circular dichroism (CD) spectra of wild-type and F^7A- and $W^{10}A$-GBAPs were recorded with a Jasco (Tokyo, Japan) J-720 spectrometer using a cuvette with a path length of 1 mm (far-UV) at 25°C. The concentration of each peptide used in the CD spectroscopy was 50 μM dissolved in 10% CH_3CN solution. CD spectra were collected with the slit width set to 1 nm, a response time of 2 s, and a scan speed of 50 nm/min. Spectra were measured three times and averaged. Ellipticity was measured from 200 to 250 nm at 1-nm intervals, corrected for a 10% CH_3CN solution baseline, and converted to molar ellipticity (θ) that is expressed as $\theta \times 10^{-3}$.

Small-molecule structure accession number. The chemical shift assignments and structural constraints have been deposited into the Biological Magnetic Resonance Data Bank under accession number 20032.

RESULTS

SAR in ring linker moiety. To address the ring linker structure required for GBAP activity, we synthesized several lactone group-substituted analogues (lactam, thiolactone, CH_2-lactone, and disulfide) (Fig. 2A). To compare the agonist activities of these analogues to that of GBAP, each peptide was assayed at 10 nM by using *E. faecalis* OU510 as the responder strain (Table 1). The use of this strain allowed us to determine the GBAP agonist activity without the additive effect of endogenously produced GBAP.

Lactam-GBAP showed a similar level of agonist activity as GBAP, while thiolactone-GBAP showed a slightly lower level of agonist activity than GBAP (Fig. 2B). CH_2-lactone-GBAP showed the same level of agonist activity as GBAP, indicating that the linker chain length is not a critical factor influencing this activity. In contrast, disulfide-GBAP lost its agonist activity, although its linker chain length was consistent with that of CH_2-lactone-GBAP (Fig. 2B). Disulfide-GBAP did not show any agonist and antagonist activities even at 1,000 nM, while $M^{11}A$-GBAP showed significant agonist activity at 100 nM (Fig. 2C); the activity corresponds to 10 nM GBAP. This suggests that the carbonyl group in the ring linker moiety but not the side chain of C-terminal residues is important for the ligand-receptor interaction.

SAR in the tail region. The SAR in the tail region was examined. A series of N-terminally truncated GBAP analogues ($desQ^1$-GBAP and $desQ^1N^2$-GBAP) were synthesized, and their GBAP agonist activities were measured. $desQ^1$-GBAP showed approximately 60% of the agonist activity exhibited by GBAP, and $desQ^1N^2$-GBAP showed no agonist activity (Fig. 3A). However, N-terminal acetylation of $desQ^1N^2$-GBAP (Ac-$desQ^1N^2$-GBAP) partially restored its agonist activity, suggesting that the amide bond at the N-terminal side of Ser^3 is the minimum recognition unit for the agonist activity. The antagonist activity of $desQ^1N^2$-GBAP against GBAP was also examined. *E. faecalis* OU510 was incubated in THB medium containing 10, 100, or 1,000 nM of $desQ^1N^2$-GBAP in the presence of 10 nM GBAP, and the induced gelatinase activity was measured. For the negative control, no $desQ^1N^2$-GBAP was added to the medium. As a result, no inhibitory effect of the addition

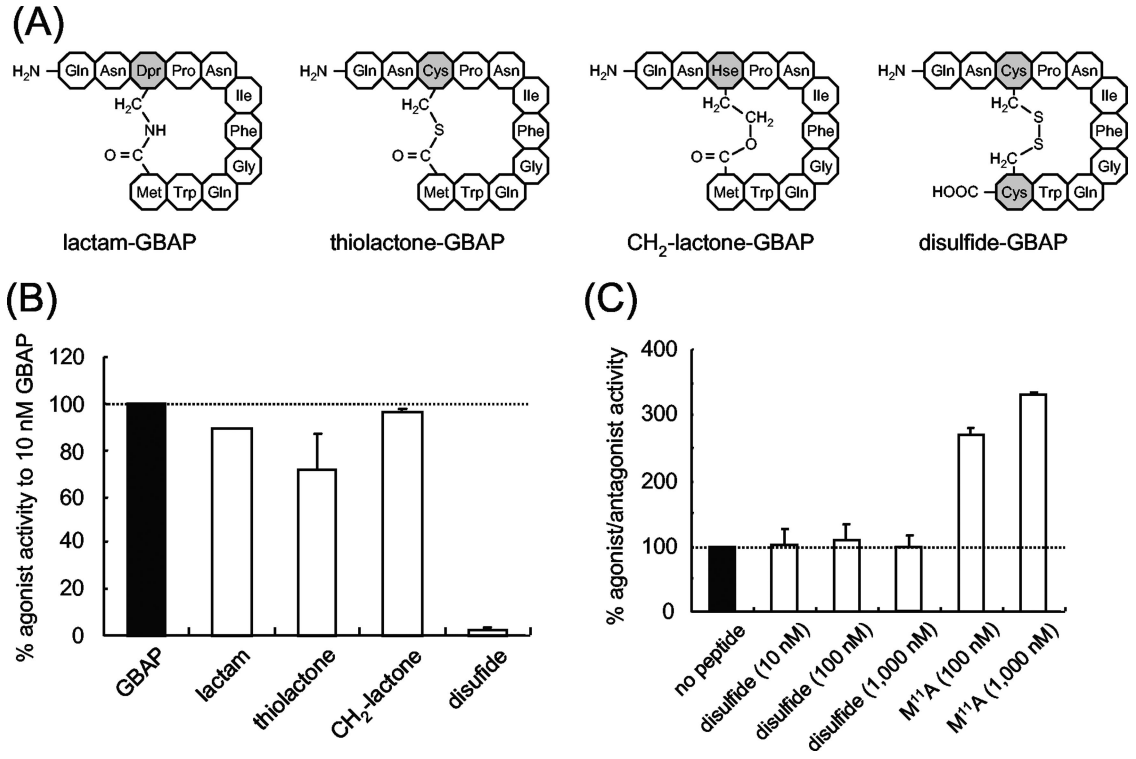

FIG. 2. SAR in the ring linker moiety. (A) Structures of a series of ring linker-substituted analogues used in this study. Dpr, diaminopropionic acid; Hse, homoserine. (B) GBAP agonist activity of the ring linker-substituted analogues. *E. faecalis* OU510 was cultured for 5 h in the presence of 10 nM each synthetic peptide, and the induced gelatinase activity in the culture supernatant was measured as GBAP agonist activity by azocoll assay according to a previously described protocol (20, 26). The activity of 10 nM GBAP (black bar) was determined to normalize the agonist activity of each peptide. The averages ± standard deviations of duplicate determinations are presented. (C) GBAP agonist/antagonist activity of disulfide-GBAP and $M^{11}A$-GBAP. Activity higher than 100% means agonist activity, and activity lower than 100% means antagonist activity. *E. faecalis* OG1RF was cultured for 5 h in the presence of various concentrations of each synthetic peptide. For the control, the induced gelatinase activity was measured in the strain cultured without the addition of exogenous peptide (black bar) and was used to normalize the agonist/antagonist activity of each peptide. The induced gelatinase activity in the culture supernatant was measured by azocoll assay. The averages ± standard deviations of duplicate determinations are presented.

of $desQ^1N^2$-GBAP was observed, indicating that $desQ^1N^2$-GBAP has no antagonist activity (Fig. 3B).

Next, we performed alanine substitutions in the tail amino acids. Three analogues (Q^1A-, N^2A-, and Q^1A-N^2A-GBAPs) were synthesized, and their agonist activities were measured (Fig. 3A). These alanine substitutions did not affect their agonist activities, indicating that the side chains in the tail amino acids are not involved in GBAP agonist activity.

SAR in the ring region. Except for Ser^3, which was involved in the formation of the lactone linkage, all the amino acid

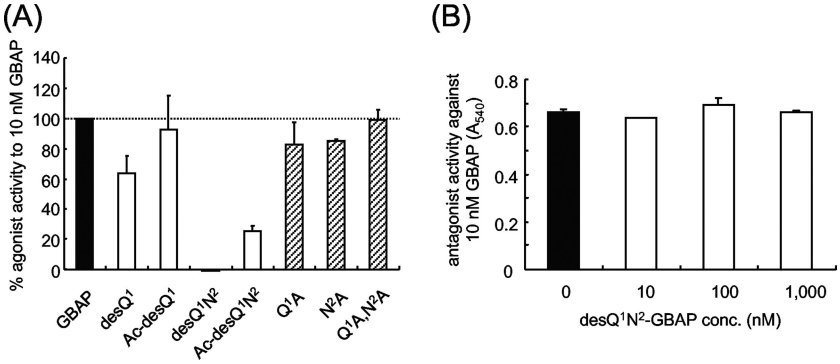

FIG. 3. SAR in the tail region. (A) GBAP agonist activity of the N-terminally truncated analogues (white bar) and alanine-substituted analogues (shaded bar). The activity of each 10 nM synthetic peptide was measured and normalized to that of 10 nM GBAP (black bar), as described in the legend of Fig. 2B. The averages ± standard deviations of duplicate determinations are presented. (B) GBAP antagonist activity of $desQ^1N^2$-GBAP. *E. faecalis* OU510 was cultured for 5 h in THB medium containing 0 nM (negative control [black bar]), 10 nM, 100 nM, or 1,000 nM of $desQ^1N^2$-GBAP in the presence of 10 nM of GBAP. The averages ± standard deviations of duplicate determinations are presented.

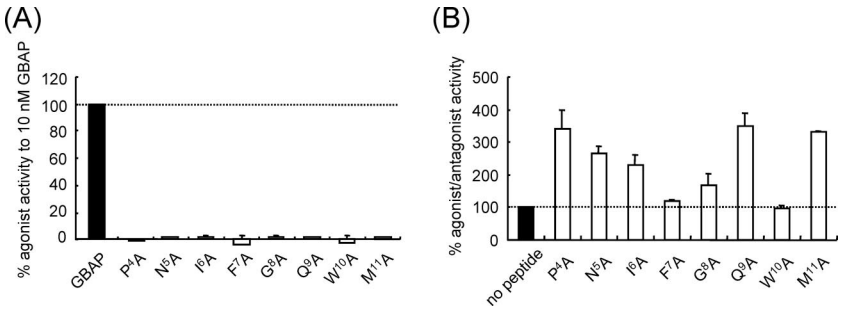

FIG. 4. SAR in the ring region. (A) GBAP agonist activities of alanine-substituted analogues. The activity of each 10 nM synthetic peptide was measured and normalized to that of 10 nM GBAP (black bar) as described in the legend of Fig. 2B. The averages ± standard deviations of duplicate determinations are presented. (B) GBAP agonist/antagonist activity of alanine-substituted analogues. Activity higher than 100% means agonist activity, and activity lower than 100% means antagonist activity. *E. faecalis* OG1RF was cultured for 5 h in the presence of 1,000 nM of each synthetic peptide. For the control, the induced gelatinase activity was measured in the strain cultured without the addition of exogenous peptide (black bar) and was used to normalize the agonist/antagonist activity of each peptide. The induced gelatinase activity in the culture supernatant was measured by an azocoll assay. The averages ± standard deviations of duplicate determinations are presented.

residues in the ring region were subjected to alanine scanning (Fig. 1). The GBAP agonist assay revealed that all the alanine-substituted analogues showed almost no activity at 10 nM, indicating that the whole structure of the ring region is crucial for GBAP agonist activity (Fig. 4A).

Next, an agonist/antagonist assay was performed for these alanine-substituted analogues at a 100-fold-higher concentration (1,000 nM) by using *E. faecalis* OG1RF as the responder strain. As shown in Fig. 4B, none of the analogues exhibited antagonist activity, whereas except for F^7A- and W^{10}A-GBAPs, all analogues showed marked agonist activities at 1,000 nM. W^{10}A-GBAP did not show any agonist activity, while F^7A-GBAP showed very weak agonist activity at 1,000 nM. These findings suggest that two aromatic amino acids, Phe^7 and Trp^{10}, are key residues for receptor interaction and activation; notably, Trp^{10} is essential for the agonist activity.

SAR at Trp^{10}. In order to investigate the function of the essential residue Trp^{10} in more detail, it was substituted with natural and unnatural aromatic amino acids. To evaluate the hydrophobicity of each peptide, the retention times of these aromatic analogues by RP-HPLC were examined (Fig. 5). Except for the tyrosine-substituted analogue (W^{10}Y-GBAP), the retention times of all other aromatic analogues were longer than that of GBAP, indicating that the hydrophobicity of these aromatic analogues was higher than that of GBAP. Subsequently, the agonist activity of each aromatic analogue was measured at various concentrations (Fig. 5). Almost all aromatic analogues showed significant agonist activity at 1,000 nM. The 1-naphtylalanine-substituted analogue (Nal^1-GBAP), the 3-benzothienylalanine-substituted analogue (Bal^3-GBAP), and the phenylalanine-substituted analogue (W^{10}F-GBAP) in particular showed the same level of agonist activity as GBAP at each concentration. W^{10}Y-GBAP showed significantly lower levels of agonist activity at all concentrations tested. On the other hand, the pentafluorophenylalanine-substituted analogue (Phe^{f5}-GBAP) and the cyclohexylalanine-substituted analogue (Cha-GBAP) showed no agonist activity regardless of their high level of hydrophobicity. Furthermore, Phe^{f5}-

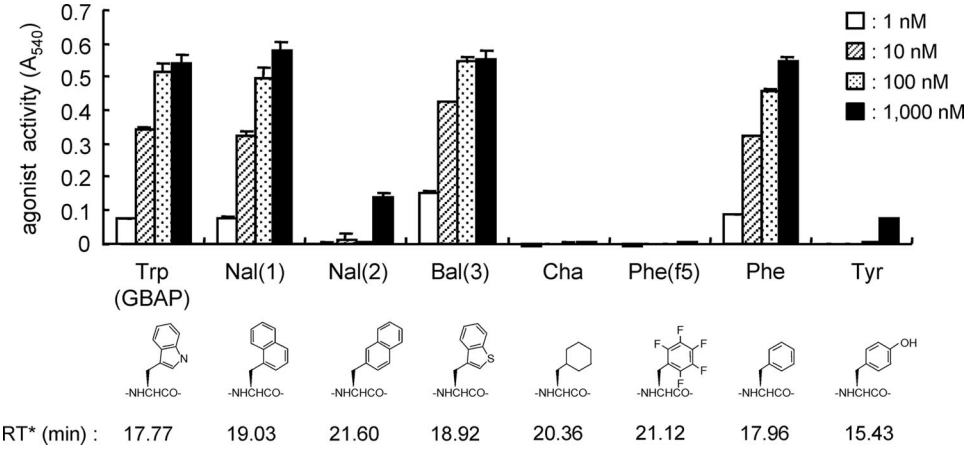

FIG. 5. SAR of Trp^{10} position. Shown are the structures, hydrophobicities, and GBAP agonist activities of Trp^{10}-substituted analogues. The induced gelatinase activities of various concentrations (1, 10, 100, and 1,000 nM) of each synthetic peptide were measured as described in the legend of Fig. 2B. Data for duplicate determinations were averaged (± standard deviations). RT, retention time of each Trp^{10}-substituted analogue in RP-HPLC. All synthetic peptides were eluted by RP-HPLC, along with a linear gradient from 20% to 60% of the CH_3CN concentration for 40 min.

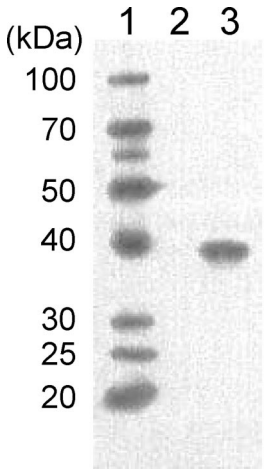

FIG. 6. Western blot analysis of FsrC-His_6. *Lactococcus lactis* NZ9000 cells were cultured in the presence of 10 ng ml^{-1} of nisin A. After induction for 3 h, the membrane fraction was prepared as described in Materials and Methods and analyzed by Western blot analysis with anti-hexahistidine tag antibody. Lane 1, XL-Ladder marker (low range); lane 2, *L. lactis* NZ9000 harboring pNZ8048 (vector control); lane 3, *L. lactis* NZ9000 harboring pNZfsrC-his6.

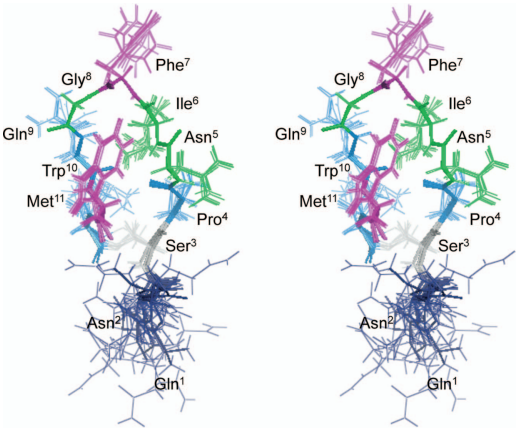

FIG. 8. Solution structure of GBAP at pH 6.0 and 10°C determined by two-dimensional proton NMR. The structure calculations of GBAP were performed by using the programs CYANA and CNS with 105 distance restraints and 8 ϕ angle restraints. A stereo view of an ensemble of the 10 lowest-energy structures is presented.

GBAP and Cha-GBAP showed no agonist/antagonist activity at all (data not shown), suggesting that the negative electrostatic potential due to the π-electron cloud on the aromatic ring surface, and not hydrophobicity, is important for receptor binding and/or receptor activation.

Receptor-binding activity of the GBAP analogues. Receptor-binding assays were developed to analyze the receptor-binding activities of the GBAP analogues. First, a receptor gene, *fsrC*, was heterologously overexpressed using *Lactococcus lactis* as the host. As shown in Fig. 6, FsrC was confirmed in the membrane fraction of recombinant *L. lactis* cells. Next, GBAP was labeled at the N terminus with FITC. Fluorescence-labeled GBAP (flu-GBAP) showed almost the same level of agonist activity as GBAP (Fig. 7A). This agrees with a previous finding that the acetylation of the α-amino group at the N terminus does not greatly influence the GBAP agonist activity (27). flu-GBAP was incubated with FsrC-overexpressing cells, and

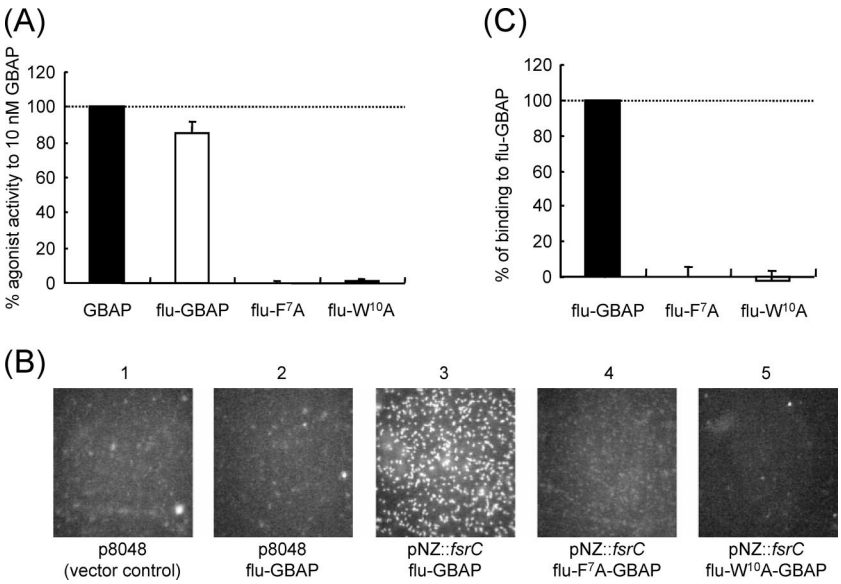

FIG. 7. Fluorescence-based receptor-binding assays. (A) GBAP agonist activity of fluorescence-labeled peptides. The activity of each fluorescence-labeled peptide was measured and normalized to that of 10 nM GBAP (black bar) as described in the legend of Fig. 2B. The averages ± standard deviations of duplicate determinations are presented. (B) Fluorescent microscopy of *L. lactis* transformants incubated with fluorescence-labeled peptides: 1, vector control cells; 2, vector control cells incubated with flu-GBAP; 3 to 5, FsrC-overexpressing cells incubated with flu-GBAP (3), flu-F^7A-GBAP (4), and flu-W^{10}A-GBAP (5). (C) Quantification of fluorescence-labeled peptides bound to the cell surface of *L. lactis* transformants. The fluorescence intensity of each fluorescence-labeled peptide was measured as described in Materials and Methods. The fluorescence intensity of each peptide was normalized to that of flu-GBAP (black bar), and the averages ± standard deviations of duplicate determinations were calculated.

TABLE 2. Structural statistics for the 10 structures of GBAP

Statistic	Value
NOE-derived distance restraints	
Intraresidue ($\|i - j\| = 0$)	57
Sequential ($\|i - j\| = 1$)	27
Short range ($2 \leq \|i - j\| \leq 4$)	13
Long range ($\|i - j\| \geq 5$)	8
Total	105
Dihedral restraints (ϕ)	8
RMSD from ideal geometry	
Bond (Å)	0.01 ± 0.0003
Angle (°)	1.19 ± 0.07
Improper (°)	0.86 ± 0.06
RMSD from experimental restraints	
Interproton distance (Å)	0.11 ± 0.03
Dihedral (°)	0.00 ± 0.00
Mean CNS energy (kcal/mol) ± SD	
Noe	90.2 ± 4.6
Cdih	0.0 ± 0.0
vdw (repel)	47.0 ± 4.5
Total	240.8 ± 8.9
Ramachandran statistics (%)	
Most favored	48.6
Allowed	37.1
Generously allowed	14.3
Disallowed	0.0
Pairwise RMSD of atomic coordinates (Å)	
Backbone	0.20 ± 0.07
Heavy	0.79 ± 0.12

the bound peptide was monitored by fluorescent microscopy (Fig. 7B). Luminescence of cells was observed only for the FsrC-overexpressing cells, indicating specific GBAP binding to FsrC. On the other hand, flu-F^7A-GBAP and flu-W^{10}A-GBAP did not bind to the FsrC-overexpressing cells. Receptor binding was also quantified by measuring the fluorescence of the labeled cells with a fluorophotometer. In this assay, F^7A-GBAP and flu-W^{10}A-GBAP did not show significant receptor binding (Fig. 7C). This indicates that these two aromatic groups in the ring region are strongly involved in GBAP binding to FsrC.

NMR structural analysis of GBAP. Two-dimensional proton NMR spectra of GBAP were measured at pH 6.0 and 10°C, and sequential assignments were completed. The structure calculation of GBAP was performed by using the CYANA and CNS programs with 105 distance restraints and 8 ϕ angle restraints. Finally, 10 structures with the lowest energy in the CNS program were chosen to represent the solution structure of GBAP (Fig. 8). An ensemble of the 10 structures exhibited CNS total energies of 240.8 ± 8.9 kcal/mol and root mean square deviations (RMSDs) of 0.20 ± 0.07 Å (backbone atoms) and 0.79 ± 0.12 Å (all heavy atoms) in the GBAP ring region. The structural statistics are summarized in Table 2. GBAP adopted a hairpin-like fold where Phe^7 and Gly^8 formed a distorted β-turn. The peptide backbone of the ring region was rigid, while that of the tail region was flexible. The side chain of Phe^7 was extended to the solvent and freely rotating. The side chain of Trp^{10} was partially buried inside the ring and fixed. Indeed, a series of NOEs were observed between the indole proton of Trp^{10} and the methylene proton of Asn^5.

Comparison of spectral properties of F^7A-GBAP and W^{10}A-GBAP to those of wild-type GBAP. In order to briefly compare the secondary structures of two inactive analogues, F^7A- and W^{10}A-GBAPs, to that of GBAP, CD spectra of the three peptides were measured (Fig. 9). Wild-type GBAP and F^7A-GBAP exhibited a negative band at 215 nm. This band was suspected to reflect the β-turn structure as observed in the cyclic hexapeptide D-Ala–L-Ala–L-Ala–D-Ala–D-Ala–L-Ala (2). On the other hand, W^{10}A-GBAP did not show any band in the far-UV region. This suggests that F^7A-GBAP retains the same secondary structure as wild-type GBAP, whereas W^{10}A-GBAP does not.

Comparison of the tertiary structure among three peptides was performed by ^1H-^{15}N heteronuclear NMR spectroscopy. Figure 10 shows the overlaid spectra of those three peptides. Several minor cross-peaks were observed in the spectrum of W^{10}A-GBAP, indicating that W^{10}A-GBAP forms multiple conformations. In contrast, only one set of cross-peaks was observed in those of wild-type GBAP and F^7A-GBAP. Except for amides of Asn^2 in wild-type GBAP and F^7A-GBAP, all one-bond ^1H-^{15}N couplings were detected as cross-peaks. The chemical shifts from F^7A-GBAP were mostly close to those of the corresponding atoms in wild-type GBAP, whereas those from W^{10}A-GBAP were totally different from those of wild-type GBAP. Since chemical shifts of amide protons and nitrogens reflect the chemical environment of their atoms in the solution, their differences between wild-type GBAP and analogues suggest a difference in peptide backbone conformations. Taken together, F^7A-GBAP, but not W^{10}A-GBAP, retained the conformation of wild-type GBAP.

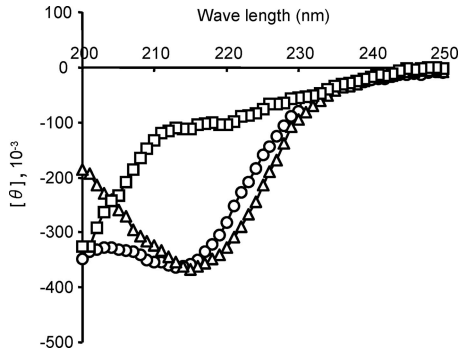

FIG. 9. CD spectra of wild-type GBAP (circle), F^7A-GBAP (triangle), and W^{10}A-GBAP (square). All peptide concentrations employed were 50 μM dissolved in 10% CH_3CN solution. Data were corrected for a 10% CH_3CN solution baseline. The path length and resolution were 1 mm and 1 nm, respectively. Spectra were measured three times and averaged.

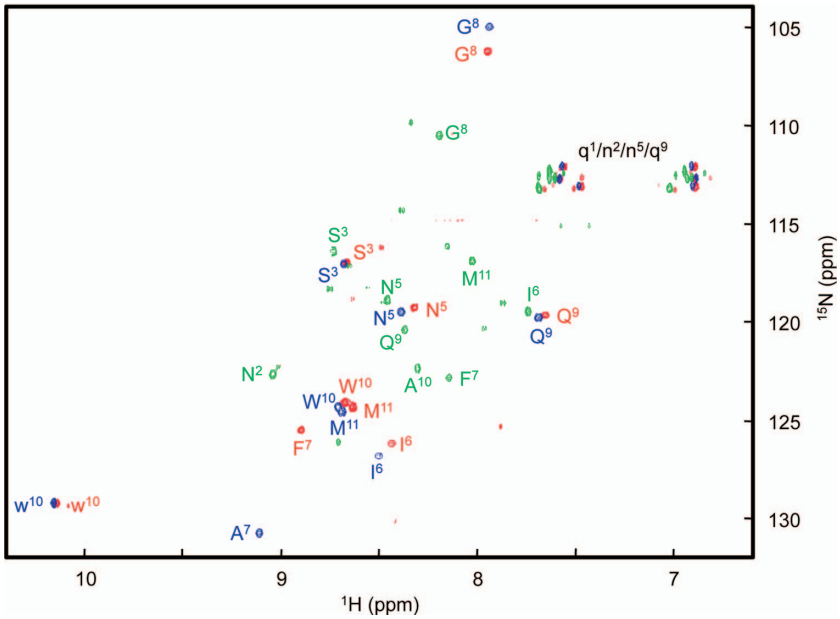

FIG. 10. Overlaid ^{1}H-^{15}N HSQC spectra of wild-type GBAP (red), F^{7}A-GBAP (blue), and W^{10}A-GBAP (green). Amino acid codes in uppercase type indicate cross-peaks for peptide backbone H-Ns, whereas those in lowercase type indicate side-chain H-N (w^{10}) and H_2-Ns (q^{1}/n^{2}/n^{5}/q^{9}) (black), respectively. In the case of W^{10}A-GBAP, only the major component is labeled. The cross-peaks of Asn^{2} from wild-type GBAP and F^{7}A-GBAP were not observed because of their low signal intensities.

DISCUSSION

This SAR study demonstrated the following: (i) the carbonyl group at the ring linker moiety is essential for the GBAP agonist activity (Fig. 2B and C); (ii) the side chain of the tail residues is not involved in the agonist activity, and an amide bond at the N-terminal side of Ser^{3} is the minimum recognition unit for GBAP agonist activity (Fig. 3); and (iii) the entire ring region is involved in the agonist activity, and notably, two aromatic residues, Phe^{7} and Trp^{10}, are strongly involved in the receptor-ligand interaction (Fig. 4, 5, and 7). With regard to the role of the side chains in the tail residues, staphylococcal AIP differs from GBAP, since the tail region is also important for inducer activity in staphylococcal AIP. However, N-terminally truncated AIP-II and AIP-IV, when present in nM concentrations, antagonized all four groups of AIPs (18, 19). On the other hand, N-terminally truncated GBAP (desQ^{1}N^{2}-GBAP) at 1 μM could not antagonize the GBAP activity (Fig. 3B). These discrepancies suggest that the molecular interaction mechanism between AIP and AgrC does not correspond to that between GBAP and FsrC.

To examine the receptor-binding activity of GBAP independent of its physiological activity, we constructed new fluorescence-based receptor-binding assay systems by using fluorescent microscopy and a fluorophotometer, which can be used to detect ligand binding to FsrC. In both fluorescent microscopy and fluorophotometer assays, it was clearly shown that flu-GBAP specifically bound onto FsrC-overexpressing cells (Fig. 7B), suggesting that these assay systems were useful for examining ligand-receptor interactions. In these assays, flu-F^{7}A-GBAP and flu-W^{10}A-GBAP showed no binding to FsrC-overexpressing cells (Fig. 7B and C). Considering this and the data for physiological activity, we conclude that these two aromatic amino acids are key residues for the GBAP-FsrC interaction.

Trp^{10} could be substituted with certain natural and unnatural aromatic amino acids without a loss of agonist activity, while Cha-GBAP showed no agonist activity (Fig. 5). This indicates that the π-electron cloud on the aromatic ring surface is important for the agonist activity. Furthermore, we showed that Phe^{f5}-GBAP, which carries a positively charged π-electron cloud, lost its agonist activity, suggesting the importance of a negative electrostatic potential on the aromatic ring surface (Fig. 5). This was also indicated by the fact that W^{10}Y-GBAP, which carries a π-electron cloud with less negative charge, showed a much lower agonist activity.

The NMR structural analysis revealed that the ring region of GBAP adopted a hairpin-like fold and was tightly packed into a compact form (Fig. 8). In Fig. 11, each residue is colored according to their relative importances for the agonist activity. It was feasible that residues classified into each category were clustered. Notably, two aromatic residues, Phe^{7} and Trp^{10}, colored purple, appeared to be important for the receptor-ligand interaction, as supported by both biological and binding activity assays. Of the two important aromatic residues, the side chain of Phe^{7} was extended outside the ring and was probably directly involved in receptor binding. On the other hand, the side chain of Trp^{10} was partially buried inside the ring region and contributed to the stabilization of the compact form, probably in addition to the direct receptor binding (Fig. 8, 9, and 10).

In this study, we have gained some knowledge on the SAR of GBAP in the context of its biological activity and receptor-binding property by using our newly constructed receptor-binding assay systems. Interestingly, the molecular interaction

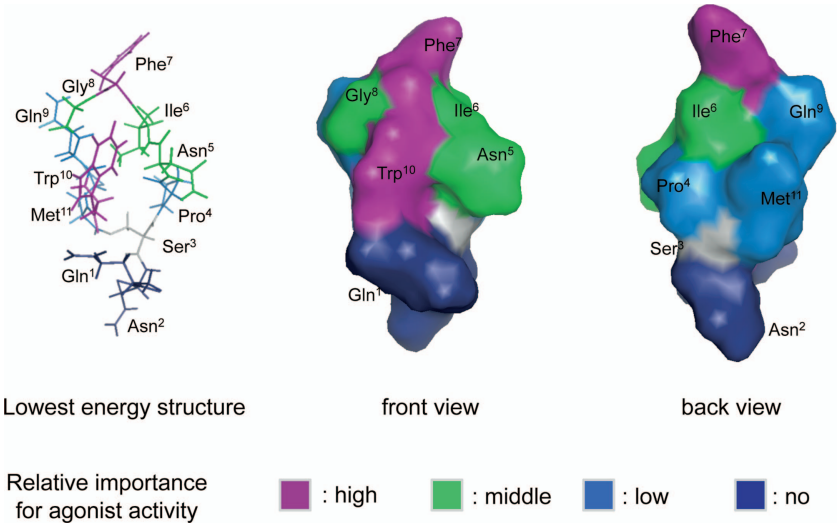

FIG. 11. Surface representation of the lowest-energy structure. Left, front view of the lowest-energy structure (Trp^{10} side view) by stick representation; center, front view; right, back view. Color coding of each residue was done according to their relative importance for the agonist activity.

mechanism between GBAP and FsrC does not correspond to that between AIPs and AgrC in staphylococci, suggesting that a rational design of staphylococcal AIP antagonist cannot directly be applied for the development of a GBAP antagonist. We also gained insight into the tertiary structure of GBAP, in which Trp^{10} is a key residue to retain the compact ring formation. The total pharmacophore information obtained in this study should be applied to the further development of the peptide-based rational design of GBAP antagonists.

ACKNOWLEDGMENTS

This work was supported in part by grants-in-aid for scientific research from the Japan Society for the Promotion of Science (grants 15580065 and 17580068 to J. Nakayama); from the Ministry of Education, Culture, Sports, and Technology of Japan (grant 16087203 to K. Nagata); from the Kato Memorial Bioscience Foundation (to J. Nakayama); and from the Waksman Foundation of Japan (to J. Nakayama).

REFERENCES

1. **Bjarnsholt, T., and M. Givskov.** 2008. Quorum sensing inhibitory drugs as next generation antimicrobials: worth the effort? Curr. Infect. Dis. Rep. **10:**22–28.
2. **Brahms, S., and J. Brahms.** 1980. Determination of protein secondary structure in solution by vacuum ultraviolet circular dichroism. J. Mol. Biol. **138:** 149–178.
3. **Brunger, A. T., P. D. Adams, G. M. Clore, W. L. DeLano, P. Gros, R. W. Grosse-Kunstleve, J. S. Jiang, J. Kuszewski, M. Nilges, N. S. Pannu, R. J. Read, L. M. Rice, T. Simonson, and G. L. Warren.** 1998. Crystallography and NMR system: a new software suite for macromolecular structure determination. Acta Crystallogr. D Biol. Crystallogr. **54:**905–921.
4. **Chang, C. D., and J. Meienhofer.** 1978. Solid-phase peptide synthesis using mild base cleavage of N alpha-fluorenyloxycarbonylamino acid, exemplified by a synthesis of dihydrosomatostatin. Int. J. Pept. Protein Res. **11:**246–249.
5. **Coburn, P. S., and M. S. Gilmore.** 2003. The *Enterococcus faecalis* cytolysin: a novel toxin active against eukaryotic and prokaryotic cells. Cell. Microbiol. **5:**661–669.
6. **Delaglio, F., S. Grzesiek, G. W. Vuister, G. Zhu, J. Pfeifer, and A. Bax.** 1995. NMRPipe: a multidimensional spectral processing system based on UNIX pipes. J. Biomol. NMR **6:**277–293.
7. **DeLano, W. L.** 2002. The PyMOL molecular graphics system. http://www.pymol.org.
8. **deRuyter, P. G. G. A., O. P. Kuipers, and W. M. de Vos.** 1996. Controlled gene expression system for *Lactococcus lactis* with the food-grade inducer nisin. Appl. Environ. Microbiol. **62:**3662–3667.
9. **Dunny, G. M., B. L. Brown, and D. B. Clewell.** 1978. Induced cell aggregation and mating in *Streptococcus faecalis*: evidence for a bacterial sex pheromone. Proc. Natl. Acad. Sci. USA **75:**3479–3483.
10. **Fujita, N., M. Yoshimura, T. Komori, and Y. Ike.** 1998. First report of the isolation of high-level vancomycin-resistant *Enterococcus faecium* from a patient in Japan. Antimicrob. Agents Chemother. **42:**2150.
11. **Geisinger, E., E. A. George, T. W. Muir, and R. P. Novick.** 2008. Identification of ligand specificity determinants in AgrC, the *S. aureus* quorum sensing receptor. J. Biol. Chem. **283:**8930–8938.
12. **Goddard, T. D., and D. G. Kneller.** SPARKY. http://www.cgl.ucsf.edu/home/sparky.
13. **Gok, E., and S. Olgaz.** 2004. Binding of fluorescein isothiocyanate to insulin: a fluorimetric labeling study. J. Fluoresc. **14:**203–206.
14. **Güntert, P.** 2004. Automated NMR structure calculation with CYANA. Methods Mol. Biol. **278:**353–378.
15. **Hancock, L. E., and M. S. Gilmore.** 1999. Pathogenicity of enterococci, p. 251–258. *In* V. A. Fischetti, R. P. Novick, J. J. Ferretti, D. A. Portnoy, and J. I. Rood (ed.), Gram-positive pathogens. ASM Press, Washington, DC.
16. **Holo, H., and I. F. Nes.** 1989. High-frequency transformation, by electroporation, of *Lactococcus lactis* subsp. *cremoris* grown with glycin in osmotically stabilized media. Appl. Environ. Microbiol. **55:**3119–3123.
17. **Kuipers, O. P., P. G. G. A. de Ruyter, M. Kleerebezem, and W. M. de Vos.** 1998. Quorum sensing-controlled gene expression in lactic acid bacteria. J. Biotechnol. **64:**15–21.
18. **Lyon, G. J., P. Mayville, T. W. Muir, and R. P. Novick.** 2000. Rational design of a global inhibitor of the virulence response in *Staphylococcus aureus*, based in part on localization of the site of inhibition to the receptor-histidine-kinase, AgrC. Proc. Natl. Acad. Sci. USA **97:**13330–13335.
19. **Lyon, G. J., J. S. Wright, T. W. Muir, and R. P. Novick.** 2002. Key determinants of receptor activation in the *agr* autoinducing peptides of *Staphylococcus aureus*. Biochemistry **41:**10095–10104.
20. **Makinen, P. L., D. B. Clewell, F. An, and K. Makinen.** 1989. Purification and substrate specificity of a strongly hydrophobic extracellular metalloendopeptidase ("gelatinase") from *Streptococcus faecalis* (strain OG1-10). J. Biol. Chem. **264:**3325–3334.
21. **Marothi, Y. A., H. Agnihotri, and D. Dubey.** 2005. Enterococcal resistance—an overview. Indian J. Med. Microbiol. **23:**214–219.
22. **Martin, C. A., A. D. Hoven, and A. M. Cook.** 2008. Therapeutic frontiers: preventing and treating infectious diseases by inhibiting bacterial quorum sensing. Eur. J. Clin. Microbiol. Infect. Dis. **27:**635–642.
23. **Mayville, P., G. Ji, R. Beavis, H. Yang, M. Goger, R. P. Novick, and T. W. Muir.** 1999. Structure-activity analysis of synthetic autoinducing thiolactone peptides from *Staphylococcus aureus* responsible for virulence. Proc. Natl. Acad. Sci. USA **96:**1218–1223.
24. **Mundy, L. M., D. F. Sahm, and M. Gilmore.** 2000. Relationships between enterococcal virulence and antimicrobial resistance. Clin. Microbiol. Rev. **13:**513–522.
25. **Murray, B. E.** 2000. Vancomycin-resistant enterococcal infections. N. Engl. J. Med. **342:**710–721.
26. **Nakayama, J., Y. Cao, T. Horii, S. Sakuda, A. Akkermans, W. M. de Vos, and H. Nagasawa.** 2001. Gelatinase biosynthesis-activating pheromone: a peptide

lactone that mediates a quorum sensing in *Enterococcus faecalis*. Mol. Microbiol. **41:**145–154.
27. **Nakayama, J., Y. Cao, T. Horii, S. Sakuda, and H. Nagasawa.** 2001. Chemical synthesis and biological activity of the gelatinase biosynthesis-activating pheromone of *Enterococcus faecalis* and its analogs. Biosci. Biotechnol. Biochem. **65:**2322–2325.
28. **Nakayama, J., S. Chen, N. Oyama, K. Nishiguchi, E. A. Azab, E. Tanaka, R. Kariyama, and K. Sonomoto.** 2006. Revised model for *Enterococcus faecalis fsr* quorum-sensing system: the small open reading frame *fsrD* encodes the gelatinase biosynthesis-activating pheromone propeptide corresponding to staphylococcal AgrD. J. Bacteriol. **188:**8321–8326.
29. **Nakayama, J., E. Tanaka, R. Kariyama, K. Nagata, K. Nishiguchi, R. Mitsuhara, Y. Uemura, M. Tanokura, H. Kumon, and K. Sonomoto.** 2007. Siamycin attenuates *fsr* quorum sensing mediated by a gelatinase biosynthesis-activating pheromone in *Enterococcus faecalis*. J. Bacteriol. **189:**1358–1365.
30. **Otto, M.** 2004. Quorum-sensing control in staphylococci—a target for antimicrobial drug therapy? FEMS Microbiol. Lett. **24:**135–141.
31. **Qin, X., K. V. Singh, G. M. Weinstock, and B. E. Murray.** 2000. Effects of *Enterococcus faecalis fsr* gene on production of gelatinase and a serine protease and virulence. Infect. Immun. **68:**2579–2586.
32. **Qin, X., K. V. Singh, G. M. Weinstock, and B. E. Murray.** 2001. Characterization of *fsr*, a regulator controlling expression of gelatinase and serine protease in *Enterococcus faecalis* OG1RF. J. Bacteriol. **183:**3372–3382.
33. **Smith, R. S., and B. H. Iglewski.** 2003. *Pseudomonas aeruginosa* quorum sensing as a potential antimicrobial target. J. Clin. Investig. **12:**1460–1465.
34. **Tendolkar, P. M., A. S. Baghdayan, and N. Shankar.** 2003. Pathogenic enterococci: new developments in the 21st century. Cell. Mol. Life Sci. **60:**2622–2636.
35. **Wüthrich, K.** 1986. NMR of proteins and nucleic acids. John Wiley & Sons, New York, NY.